Flux Pinning Docking Interfaces in Satellites Using Superconducting Foams as Trapped Field Magnets

Michael R. Koblischka, *Member, IEEE*, Anjela Koblischka-Veneva, Denis Gokhfeld, S. Pavan Kumar Naik, Quentin Nouailhetas, Kévin Berger, and Bruno Douine

***Abstract*—Flux-Pinning Docking Interfaces (FPDI) in satellite systems were developed using bulk superconductors and permanent magnets in previous works. However, such FPDIs have limited magnetic field strength, consist of heavy-weight material, and can only be used with a single purpose, i.e., as chasing or docking satellite. Replacing the magnetic material in the FPDI by a trapped field (TF)-magnet would enable the interface to operate for both purposes, i.e., generating a (stronger) magnetic field and trapping it. We show the requirements for such a system and discuss the possible gains when using a TF-FPDI in satellites. To reduce the system weight, the use of superconducting foams as superconducting material is discussed in detail. Furthermore, the use of superconducting foams, the size of which can be easily upscaled, may also comprise the function of the damping material, so even more weight could be saved for the payload.**

***Index Terms*—Flux-pinning docking interface, foams, trapped field magnets, YBCO.**

Fig. 1. CubeSats orbiting Earth. Figure from Ref. [7].

I. Introduction

FLUX pinning docking interfaces (FPDI) for satellite systems were designed in the literature on the base of $YBa_2Cu_3O_{7-\delta}$ (YBCO) bulks, Nd-Fe-B permanent magnets and electromagnets [1]–[5]. Coupling a superconductor to a magnet induces vortices in the superconducting material, which passively stabilize the position and orientation of the magnet, so an active control of the docking process is not required. Thus, flux pinning-based docking systems are especially interesting for cube satellites (CubeSats, see Fig. 1), which are small satellite systems providing affordable access to space for small companies, research institutes and universities [6], [7]. The modular design enables that subsystems can be stacked together according to the needs of the mission, which demands a simple, effective and remote-controlled docking system. For this purpose, the FPDI system is well suited. However, operating a real FPDI with two superconductor pellets to trap fields from (small) Nd-Fe-B permanent magnets, only a weak stiffness of few N/m can be obtained [1], [5]. While the stability, controlability, and the dynamic force characteristics of such systems were modelled extensively [8]–[13], the role of the materials employed was left completely undiscussed, using typical samples of Nd-Fe-B disks (30 mm diameter, ~0.5 T surface field) and bulk, superconducting YBCO disks (30 mm diameter, operating at 77 K with 0.3 T trapped field). However, there has been considerable development on the material side in the recent years, and as the weight of the FPDI and its operational requirements are limiting the available payload of the satellite, this is an important question to be answered.

Bulk superconducting materials (see Fig. 2(a) are currently employed for levitation, in electric motors and generators or as trapped field (TF) magnets (superconducting permanent magnets), which can be much stronger as any permanent magnet material [14]. For applications operating at liquid nitrogen temperature (77 K), YBCO is the material of choice due to its superior properties at elevated temperatures [15].

A record trapped field of 17.6 T at 26 K was reached in the literature, measured in between a stack of two melt-textured YBCO bulk samples (25 mm diameter) [16], [17], closely followed by others employing differently processed bulks using infiltration growth (IG) [18] and stacks of YBCO tapes [19].

Manuscript received September 19, 2021; revised December 24, 2021; accepted January 26, 2022. Date of publication February 1, 2022; date of current version February 16, 2022. This work was supported in part by SUPERFOAM international project funded by ANR and DFG under Grants ANR-17-CE05-0030 and DFG-ANR Ko2323-10. *(Corresponding author: Michael R. Koblischka.)*

Michael R. Koblischka and Anjela Koblischka-Veneva were with the Department of Experimental Physics, Saarland University, 66041 Saarbrücken, Germany. They are now with the Shibaura Institute of Technology, Tokyo 135-8548, Japan.

Denis Gokhfeld is with the Kirensky Institute of Physics, Federal Research Center KSC SB RAS, Krasnoyarsk 660036, Russia.

S. Pavan Kumar Naik is with the Department of Physics, Tokyo University of Science, Tokyo 162-8601, Japan.

Quentin Nouailhetas is with the Department of Experimental Physics, Saarland University, 66041 Saarbrücken, Germany, and also with Université de Lorraine, GREEN, F-54000 Nancy, France.

Kévin Berger and Bruno Douine are with Université de Lorraine, GREEN, F-54000 Nancy, France.

Color versions of one or more figures in this article are available at https://doi.org/10.1109/TASC.2022.3147734.

Digital Object Identifier 10.1109/TASC.2022.3147734

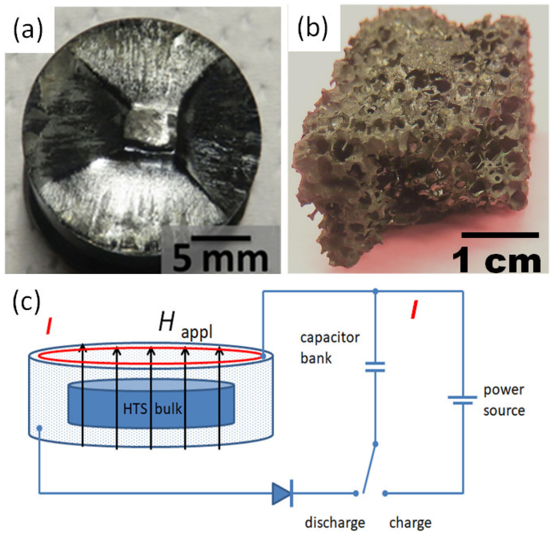

Fig. 2. (a) IG-processed bulk sample with 2 cm diameter. (b) Superconducting YBCO foam, with dimensions 5 × 2 × 2 cm^3, porosity 40 PPI. (c) Schematic sketch of the best suited energizing method for bulks, the pulsed-field magnetization (PFM).

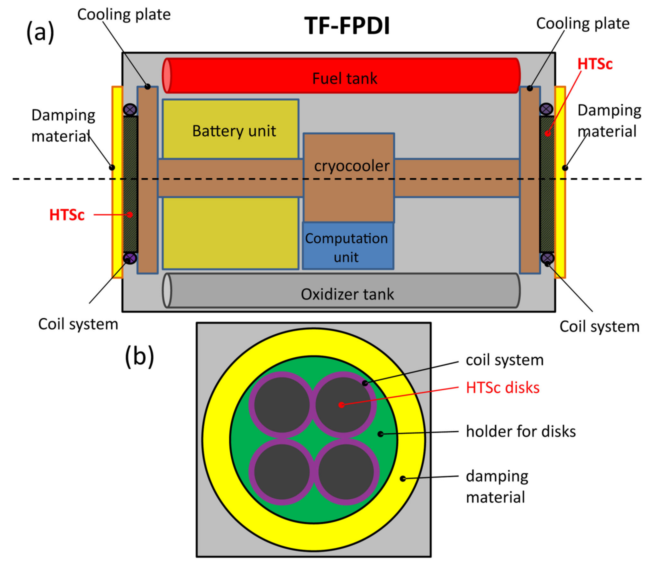

Fig. 3. (a) Schematic drawing of a TF-FPDI equipped CubeSat as side view, not to scale. (b) Front view of the FPDI showing the superconductor disks (dark grey), each enclosed in a coil system (drawn in violet).

At 77 K, the trapped fields are typically around 0.4–0.5 T for a single pellet (20 mm diameter), and can reach up to 1 T when replacing Y by Gd or nonmagnetic Eu [20].

The present contribution is organized as follows: Section II gives some experimental details. In Section III, we use the concept of TF magnets to design a new type of FPDI system, and discuss the resulting changes of operation during docking and undocking. In Section IV, we discuss the material issues for TF operation and suggest the use of superconducting foams (see Fig. 2(b)) as TF magnets, which will provide a further reduction of the weight, which is of considerable interest for the satellite users as it increases the payload. Finally, in Section V, some conclusion are presented.

II. Experimental Procedures

The magnetic measurements shown were performed using a Quantum Design MPMS3 SQUID system with ±7 T applied field (field sweep rate 0.36 T/min). In all cases, the field was applied perpendicular to the flat surface of the foam struts (typical size ∼1.2 × 1 × 0.1 mm^3, no pores) or the *(a,b)*-plane of bulks (typical size ∼2 × 1.5 × 1 mm^3, cut by diamond saw 3 mm below the seed of the bulk pellet with 2 cm diameter).

High-field measurements (up to 33 T, lowest temperature 40 K) were carried out at NHFML, Nijmegen, The Netherlands, using a cantilever torque magnetometer [21]. The field sweep rate was 2 T/min. For these experiments, the sample size was further reduced by mechanical polishing to 1 × 1 × 0.5 mm^3, before glueing them to the cantilevers with G01 glue.

The TF mappings of the bulk samples (size 2 cm diameter, 1 cm height (IG-YBCO) and 5 × 2 × 2 cm^3 (YBCO foam)) were carried out using a homemade setup with a scanning Hall probe operating at 77 K and a distance of 1.5–2 mm to the sample surface [22], [23].

III. Design of FDPI With TF Magnets

The development of the superconducting TF magnets or "supermagnets" is well of importance for the design of FPDI systems. There are two main advantages for using TF magnets in FPDI systems (TF-FPDI):

1) While in the original configuration of FPDIs, a satellite must be designated either as target or chaser satellite, this distinction could be completely eliminated when using TF magnets, as the TF magnet can be energized or discharged on demand, even when being in space. Therefore, TF magnets enable a more straightforward and flexible assembly of satellite architectures in space.
2) The second advantage is the complete elimination of permanent magnets or electromagnets. Thus, TF magnets save a lot of weight and there are no problems with shielding the magnetic field while transporting the satellite.

The TF magnets can be energized by field-cooling or pulsed field magnetization (PFM), with the pulsed field magnetization [24], [25] as illustrated in Fig. 2(c) being the choice for the operation in satellites. The PFM method enables a quick (milliseconds) energizing of all superconducting elements. Additionally, a fuel cell could be used to power the coils as described in [26]. All the superconducting pellets used in the TF-FPDI must be equipped with a coil system wrapped around them [27] to allow for PFM (violet rings in Figs. 3 to 5). The coils could be made from conventional Cu wires, but as they should be also cooled down together with the superconducting pellet to be more effective, a superconducting coil (e.g., built using YBCO tapes) could be used as well for this purpose. Both the superconducting bulk and the coil system can be impregnated together using a resin as described in [16] to obtain a compact and sturdy TF unit.

As long as the energized TF magnet is kept below the superconducting transition temperature, T_c, the trapped magnetic field will stay in the sample without further consuming energy.

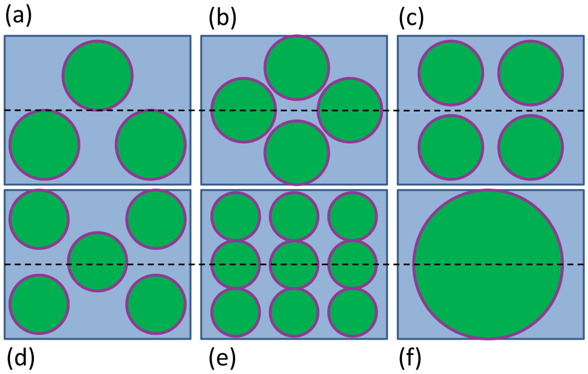

Fig. 4. (a–f) Possible arrangements of the superconducting disks for TF-FPDI systems.

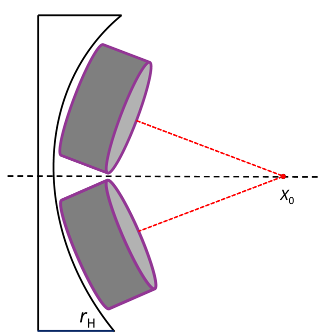

Fig. 5. Schematic drawing of a spheric arrangement (radius r_H) of the superconducting disks to improve the magnetic field strength on point X_0 on the center line. Such increased field may help the guidance of the target satellite.

Allowing the TF magnet to warm up above T_c will erase all magnetic fields. Thus, the superconductors could be activated as TF magnets when needed, or serve as field receptors (= superconductors) when being only cooled. Thus, the undocking process is now much simpler by just warming up the superconducting disks to erase all magnetic signals without trace. The docking process benefits from the possible larger magnetic fields which can be created by a TF magnet as a higher field will introduce more vortices in the superconductor, so the entire FPDI system will be much stiffer.

A sketch of a TF-FPDI is presented in Fig. 3(a), (b), following the basic layout of a CubeSat by Yang *et al.* [12]. Using TF-FPDIs, both ends of the satellite are equipped identically with the superconductors mounted on cooling plates as shown in (a). One cryocooler may handle both cooling plates with the superconductor elements, but for optimum use, it should be possible to warm up the superconductors independently. The front view (b) shows the superconductor elements behind and encapsulated by the damping material, which can be designed, e.g., from an Al metal foam [28], [29]. A configuration of 4 TF-magnets is drawn, which can serve to either generate magnetic fields or to trap them, depending if they are energized or not.

However, to design a proper TF-FPDI system, we must consider all properties of the superconducting material. For building up TF-magnets, a large sample size of the superconducting material is required as the maximum trapped field depends on the sample size in contrast to permanent magnets [30], [31]. On the other hand, the PFM energizing places a size limit on the TF magnets as the coils must be able to produce a magnetic field being large enough to successfully replace the permanent magnets.

YBCO bulk samples are prepared by melt-texturing [16], [17], [30] or the infiltration growth process, which provides a better control of the shape of the pellets [32]. However, obtaining large sample sizes is a difficult task as a good texture is essential to enable the flow of strong supercurrents [14]. The necessary oxygenation step when preparing YBCO leads to a phase transformation from the tetragonal phase ($\delta = 0.5...1$) to an orthorhombic phase $\delta = 0...0.5$). In this step, internal cracking may occur which limits the possible sample size [33]. Furthermore, the oxygenation time required to fully oxygenate a large, bulk sample increases tremendously; so necessary oxygenation times of 14 days and more are quite common. Therefore, superconducting samples prepared in this way are costly, and difficult to be handled as vacuum or even air may alter the oxygenation at the sample surface. Furthermore, magnetostriction plays an important role when trapping large magnetic fields [31]. Due to the forces involved, the superconductor sample may break up, and the aforementioned internal cracks strongly contribute to this. Therefore, a reinforcement by steel rings and additional polymer impregnation is required to withstand the forces as learned in the high-field experiments [16]–[18].

All the points mentioned imply that we have to make a compromise between sample size and the possible performance. Sketches of the possible arrangements of the TF-magnets are given in Fig. 4(a)–(f). Another important limitation of the sample size comes from the necessary coil system, wound around each bulk. To reach reasonably high field values, the coil systems must be kept small enough. For the FPDI, this means that configurations with 1 to 3 bulk samples are not the ones of choice; it will be better to choose an option with 4 or more disks as done in the most recent FPDI calculations by Bai *et al.* [13]. The case of one large superconducting pellet is only feasible for field trapping, and such sizes can be best reached using superconducting foam materials as discussed below. Finally, Fig. 5 presents a further refinement of the arrangement of the superconducting pellets which was not considered in the modelling yet. To increase the magnetic field on the center line (point X_0), the TF-magnets could be arranged on a spherical geometry with radius r_H describing the curvature of the sample holder. Such holder is anyway needed to fix the TF-magnets during the energizing steps. This focusing of the magnetic field on the center line of the satellite will lead a much better guidance of the chaser satellite due to the higher magnetic field experienced.

IV. Superconducting Foam as Active Element of FDPI

Having discussed the properties of the TF-FPDI system, we can now better understand where the YBCO foams as porous superconducting materials may solve some of the problems mentioned before [34], [35]. Polymer, metallic or ceramic foams as nature-inspired, bionic materials mimic the construction elements of biologic load-bearing structures like wood or bones and are nowadays used in many places in industry for various tasks, e.g., as energy absorbers in aeronautics or in car industry,

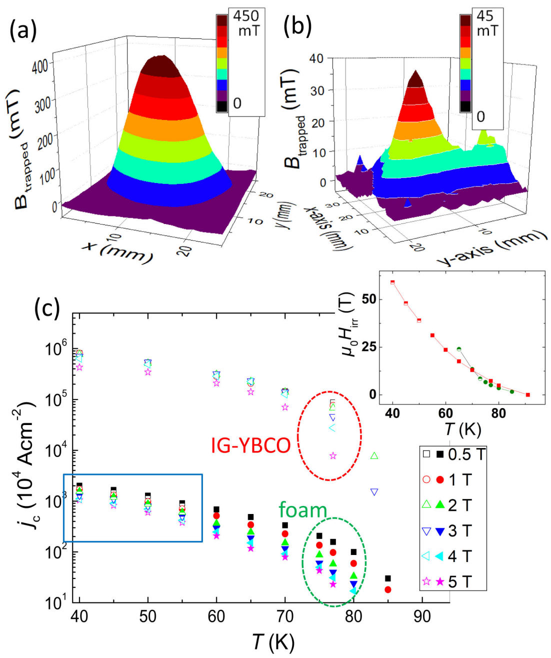

Fig. 6. TF-measurement on an (a) IG-YBCO bulk sample and (b) YBCO foam sample. Both samples are shown in Fig. 2. (c) Critical current densities as function of temperature for various applied magnetic fields of an IG-processed YBCO sample (open symbols) and of an YBCO foam struts (full symbols) as function of temperature. Extrapolated data are marked by half-filled symbols. The inset shows $B_{\rm irr}(T)$ of foam struts (●) and high-field measurements [21] of an IG-processed bulk (■) for comparison. Half-filled symbols indicate extrapolation/reconstruction of the data.

as light-weight structural damping material, as filter materials, heat exchangers and others [36], [37]. The open-porous structure of foams enables the addition of metallic layers by, e.g., electrodeposition to further improve the mechanical strength [28], [29], and the pores may be filled up with resins if needed. The big advantage of such foam-type materials is the straightforward, easy shaping of the samples and upscaling of the sample size, being only limited by the furnace dimensions [38]. YBCO foams were originally developed in [39], [40], and further developments were done in Refs. [38], [41]–[43]. The present status of the performance of YBCO foam samples as trapped field magnets was discussed previously in Refs. [22], [23].

Fig. 6(a), (b) present spatially resolved TF measurements ($B_{\rm trapped}(x, y)$) on an YBCO bulk and an YBCO foam performed at 77 K, after the sample was field-cooled by a Nd-Fe-B permanent magnet (∼0.5 T surface field). The bulk sample (a) shows a well developed single cone-shape of the trapped field 3D profile due to its single grain nature, indicating that the sample is free from structural defects. The foam sample shows a maximum, but not extending over the entire sample width and also several small, sharp maxima can be seen. It is obvious from (b) that the rectangular sample shape is not optimized for TF operation, which would be better pellet-like. The small, sharp maxima are due to local current loops being compressed when reducing the external field as discussed in [22], [41]. The TF-measurement of the foam is thus clearly affected by the porosity of the sample. Estimating the overall critical current density, j_c, from the TF data using $j_c R \propto B_{\rm trap,max}/\mu_0$ (Bean model, [44]) yields only 320 A/cm^2 for the complete porous foam structure. This implies that working at lower T will considerably improve the TF performance (higher j_c and reduced effects of granularity).

As there are no data available in the literature for $B_{\rm trapped}(x, y)$ at $T > 77$ K, Fig. 6(c) presents $j_c(T)$ for various applied magnetic fields of an IG-processed YBCO bulk. The $j_c(H)$-data of an YBCO foam strut, which contain both inter- and intragranular information (thus, j_c(foam)< j_c(bulk)), were measured down to 60 K. The $j_c(T)$-curves shown here were then obtained by extrapolation using various H^α-fits as presented in [22]. Irreversibility lines, $B_{\rm irr}(T)$, are shown in the inset to (c). Measurements of foam struts (●) were done up to 75 K, and the low-T data (half-filled symbols) are obtained via pinning force scaling [43]. All data can be fitted to the relation $H_{\rm irr}(T) = H_0(1 - T/T_c)^n$ with $n = 3$ and $H_0 = 130$ T, common for many 123-materials [45]. Data of an IG-processed YBCO bulk determined from high-field measurements (■) are presented as well. The half-filled symbols indicate incomplete loops, where $B_{\rm irr}(T)$ was reconstructed graphically. These data justify the extrapolation and demonstrate that $B_{\rm irr}(T)$ of the foam struts is comparable to that of the IG-processed bulks, being considerably larger than those of conventional YBCO bulks. However, we must note that $B_{\rm irr}(T)$ is an intragranular property.

The data presented enable to judge how $B_{\rm trapped}$ will improve on reducing T. The $B_{\rm irr}$-curves set an upper limit for field trapping as the pinning forces are zero at $B_{\rm irr}$. The $j_c(T)$-curves at 0.5 T and 1 T are the ones closest to the TF conditions. Assuming the same shape of the $j_c(T)$-curves for bulks and foams (see the extrapolated data in the blue box, open symbols), we can expect an increase of j_c by a factor of ∼20 when going to 40 K. This, together with improved seeding and an optimization of the sample shape, will contribute to a possible TF-value of ∼800 mT for an optimized foam sample. Such an increase of TF would make the foams very competitive, regarding the other advantages of reduced weight and the better cooling efficiency.

V. Conclusion

To conclude, we have presented the design of a TF-FPDI system. Using the TF magnet concept, the superconductor pellets can operate as field generators or receivers, which enables to build up more complex architectures composed of, e.g., CubeSats in space. To realize such systems, we also have shown that porous high-T_c superconductors (open-cell foams) are very promising materials for applications wherever the sample weight or the cooling efficiency counts. Thus, the superconducting foams may be a good alternative as TF-magnets for FPDIs, saving considerable weight for more payload. The achieved trapped field values of the superconducting foam samples at 77 K are currently still smaller than those of conventional bulks, but promising when operating at lower temperatures and the cooling efficiency can already well be demonstrated in the experiments.

Acknowledgment

The authors like to thank the late Prof. H. P. Roeser and Prof. S. Fasoulas (Institute for Space Systems, University of Stuttgart) for valuable discussions on the use of superconductors in space.

REFERENCES

[1] J. P. Shoer and M. A. Peck, "Flux-pinned interfaces for the assembly, manipulation, and reconfiguration of modular space systems," *J. Astron. Sci.*, vol. 57, no. 3, pp. 667–688, 2009.

[2] J. Shoer, W. Wilson, L. Jones, M. Knobel, and M. Peck, "Microgravity demonstrations of flux pinning for station-keeping and reconfiguration of CubeSat-sized spacecraft," *J. Spacecraft Rockets*, vol. 47, pp. 1066–1069, 2010.

[3] L. L. Jones and M. A. Peck, "Stability and control of a flux-pinned docking interface for spacecraft," in *Proc. AIAA Guidance, Navigation, Control Conf.*, Toronto, ON, Canada, 2010, pp. 2010–8298.

[4] W. R. Wilson and A. A. Peck, "An air-levitated testbed for flux pinning interactions at the nanosatellite scale," in *Proc. AIAA Guidance, Navigation, Control Conf.*, Toronto, ON, Canada, 2010, pp. 2010–8221.

[5] L. L. Jones, "The dynamics and control of flux-pinned space systems: Theory and experiment," Ph.D. dissertation, Cornell Univ., New York, NY, USA, 2012.

[6] CubeSat program, 2021, Accessed: Feb. 6, 2022. [Online]. Available: https://www.cubesat.org/cubesatinfo

[7] European Space Agency, 2021, Accessed: Feb. 6, 2022. [Online]. Available: https://www.esa.int/Enabling_Support/Preparing_for_the_Future/Discovery_and_Preparation/CubeSats

[8] W. J. Yang, J. Xu, L. Yu, and Y. Liu, "Experimental investigation of mechanical characteristics in superconducting interfaces for self-assembly of spacecraft modules," *Physica C*, vol. 483, pp. 173–177, 2012.

[9] Y. Lu, M. Zhang, and D. Gao, "Lateral force and lateral connection stiffness of flux pinned docking interface," *J. Supercond. Novel Magn.*, vol. 26, pp. 3027–3036, 2013.

[10] W. J. Yang, L. Yu, W. J. Yuan, and Y. Liu, "Effect of pre-magnetization on quasi-static force characteristics in a space superconducting interface structure adopting high TC superconductors," *J. Supercond. Nov. Magn.*, vol. 27, no. 1, pp. 95–100, 2014.

[11] W. J. Yang, M. Ye, J. Xu, T. Zhang, H. B. Tang, and Y. Liu, "Dynamic force characteristics in a superconducting interface module," *IEEE Trans. Appl. Supercond.*, vol. 25, no. 3, Jun. 2015, Art. no. 3700704.

[12] W. Yang, D. Liao, and L. Yao, "Effects of magnetization conditions on dynamic characteristics of spacecrafts with superconducting flux pinning docking interfaces," *J. Appl. Phys.*, vol. 124, 2018, Art. no. 213901.

[13] M. Bai, W. Yang, D. Liao, D. Song, and H. Tang, "Effect of composite superconductor structure on dynamic properties of superconducting interface and formation in space application," *J. Supercond. Novel Magn.*, vol. 33, pp. 599–607, 2020.

[14] J. H. Durrell, M. D. Ainslie, D. Zhou, P. Vanderbemden, T. Bradshaw, S. Speller, M. Filipenko, and D. A. Cardwell, "Bulk superconductors: A roadmap to applications," *Supercond. Sci. Technol.*, vol. 31, 2018, Art. no. 103501.

[15] A. Gurevich, "To use or not to use cool superconductors," *Nat. Mater.*, vol. 10, pp. 255–259, 2011.

[16] M. Tomita and M. Murakami, "High-temperature superconductor bulk magnets that can trap magnetic fields above 17 Tesla at 29 K," *Nature*, vol. 421, pp. 517–520, 2003.

[17] J. H. Durrell *et al.*, "A trapped field of 17.6 T in melt-processed bulk Gd-Ba-Cu-O reinforced with shrink-fit steel," *Supercond. Sci. Technol.*, vol. 27, 2014, Art. no. 082001.

[18] D. K. Namburi *et al.*, "A trapped field of 14.3 T in Y-Ba-Cu-O bulk superconductors fabricated by buffer-assisted seeded infiltration and growth," *Supercond. Sci. Technol.*, vol. 31, 2018, Art. no. 125004.

[19] A. Patel *et al.*, "A trapped field of 17.7 T in a stack of high temperature superconducting tape," *Supercond. Sci. Technol.*, vol. 31, 2018, Art. no. 09LT01.

[20] K. Y. Huang *et al.*, "Improved trapped field performance of single grain Y-Ba-Cu-O bulk superconductors containing artificial holes," *J. Am. Ceram. Soc.*, vol. 104, pp. 6309–6318, 2021, doi: 10.1111/jace.18017.

[21] Q. Nouailhetas *et al.*, "High-field measurements on bulk $YBa_2Cu_3O_y$ samples prepared by the Infiltration-Growth (IG) technique," presented at ISS 2019, Kyoto, Japan, poster PCP7-4, to be published.

[22] M. R. Koblischka *et al.*, "Superconducting foams as trapped field magnets," *Materials*, vol. 12, 2019, Art. no. 853.

[23] M. R. Koblischka, S. Pavan Kumar Naik, A. Koblischka-Veneva, D. Gokhfeld, and M. Murakami, "Flux creep after field trapping in $YBa_2Cu_3O_x$ foams," *Supercond. Sci. Technol.*, vol. 33, 2020, Art. no. 044008.

[24] H. Fujishiro, T. Tateiwa, A. Fujiwara, T. Oka, and H. Hayashi, "Higher trapped field over 5 T on HTSC bulk by modified pulsed field magnetizing," *Physica C*, vol. 445/448, pp. 334–338, 2006.

[25] M. D. Ainslie *et al.*, "Pulsed field magnetization of single-grain bulk YBCO processed from graded precursor powders," *IEEE Trans. Appl. Supercond.*, vol. 26, no. 4, Jun. 2016, Art. no. 6800104.

[26] M. Hinaje, S. Rael, K. Berger, R. Linares, and J. Lévêque, "The use of a small single fuel cell to feed a 10-H superconducting coil," *IEEE Trans. Appl. Supercond.*, vol. 28, no. 5, Aug. 2018, Art. no. 4902606.

[27] K. Berger *et al.*, "3D modeling of coils for pulsed field magnetization of HTS bulk pellets in an electrical machine," *IEEE Trans. Appl. Supercond.*, vol. 28, no. 4, Jun. 2018, Art. no. 6801205.

[28] A. Jung, S. Diebels, A. Koblischka-Veneva, J. Schmauch, A. Barnoush, and M. R. Koblischka, "Microstructural analysis of electrochemical coated open-cell metal foams by EBSD and nanoindentation," *Adv. Eng. Mater.*, vol. 16, pp. 15–20, 2013.

[29] A. Jung and S. Diebels, "Micromechanical characterization of metal foams," *Adv. Eng. Mater.*, vol. 19, 2019, Art. no. 1900237.

[30] R. Tournier, E. Beaugnon, and O. Belmont, "Processing of large $Y_1Ba_2Cu_3O_{7-x}$ single domains for current-limiting applications," *Supercond. Sci. Tech.*, vol. 13, pp. 886–896, 2000.

[31] T. H. Johansen, "Flux-pinning-induced stress and magnetostriction in bulk superconductors," *Supercond. Sci. Technol.*, vol. 13, pp. R121–R137, 2000.

[32] D. K. Namburi, Y.-H. Shi, and D. A. Cardwell, "The processing and properties of bulk (RE)BCO high temperature superconductors: Current status and future perspectives," *Supercond. Sci. Technol.*, vol. 34, 2021, Art. no. 053002.

[33] P. Diko, "Cracking in melt-grown RE-Ba-Cu-O single-grain bulk superconductors," *Supercond. Sci. Technol.*, vol. 17, pp. R45–R58, 2004.

[34] M. R. Koblischka and A. Koblischka-Veneva, "Porous high-T_c superconductors and their applications," *AIMS Mater. Sci.*, vol. 5, pp. 1199–1213, 2018.

[35] D. M. Gokhfeld, M. R. Koblischka, and A. Koblischka-Veneva, "Highly porous superconductors: Synthesis, research, and prospects," *Phys. Met. Metallography*, vol. 121, pp. 936–948, 2020.

[36] P. Colombo, "Ceramic foams: Fabrication, properties and applications," *Key Eng. Mater.*, vol. 206/213, pp. 1913–1918, 2002.

[37] C. Hill and J. Eastoe, "Foams: From nature to industry," *Adv. Colloid Interface Sci.*, vol. 247, pp. 496–513, 2017.

[38] J. G. Noudem and J. G. Noudem, "Development of shaping textured YBaCuO superconductors," *J. Supercond.*, vol. 24, pp. 105–110, 2011.

[39] E. S. Reddy and G. J. Schmitz, "Superconducting foams," *Supercond. Sci. Technol.*, vol. 15, pp. L21–L24, 2002.

[40] E. S. Reddy and G. J. Schmitz, "Ceramic foams," *Amer. Ceram. Soc. Bull.*, vol. 81, pp. 35–37, 2002.

[41] E. Bartolomé, X. Granados, T. Puig, X. Obradors, E. S. Reddy, and G. J. Schmitz, "Critical state in superconducting single-crystalline $YBa_2Cu_3O_7$ foams: Local versus long-range currents," *Phys. Rev. B*, vol. 70, 2004, Art. no. 144514.

[42] M. R. Koblischka, A. Koblischka-Veneva, E. S. Reddy, and G. J. Schmitz, "Analysis of the microstructure of superconducting YBCO foams by means of AFM and EBSD," *J. Adv. Ceram.*, vol. 3, pp. 317–325, 2014.

[43] M. R. Koblischka *et al.*, "Current flow and flux pinning properties of YBCO foam struts," *IEEE Trans. Appl. Supercond.*, vol. 29, no. 5, Aug. 2019, Art. no. 8001405.

[44] C. P. Bean, "Magnetization of hard superconductors," *Phys. Rev. Lett.*, vol. 8, pp. 250–253, 1962.

[45] E. Altin *et al.*, "Vortex pinning and magnetic peak effect in $Eu(Eu,Ba)_{2.125}Cu_3O_x$," *J. Mater. Sci., Mater. Electron.*, vol. 25, pp. 1466–1473, 2014.